JOURNAL OF AIRCRAFT
Vol. 31, No. 4, July–Aug. 1994

Severe Turbulence and Maneuvering from Airline Flight Records

R. C. Wingrove* and R. E. Bach Jr.†
NASA Ames Research Center, Moffet Field, California 94035

Digital flight records from reported clear-air turbulence incidents are used to determine winds and turbulence, to determine maneuver *g* loads, and to analyze control problems. Many cases of severe turbulence are found downwind of mountains and thunderstorms where sharp, sudden jolts are associated with vortices in atmospheric waves. Other cases of severe turbulence are found in strong updrafts above thunderstorm buildups that may be undetected by onboard weather radar. An important finding is that there are large maneuvering loads in over half of the reported clear-air turbulence incidents. Maneuvering loads are determined through an analysis of the short-term variations in elevator deflection and aircraft pitch angle. For altitude control in mountain waves the results indicate that small pitch angle changes with proper timing are sufficient to counter variations in vertical wind. For airspeed control in strong mountain waves, however, there is neither the available thrust nor the quickness in engine response necessary to counter the large variations in winds.

Introduction

FLIGHT incidents involving severe atmospheric disturbances are a continuing problem that must be better understood to improve safety. During the past 5 yr airline pilots have reported 96 severe-turbulence incidents.[1] In some of these incidents the large changes in *g* loads have caused injuries to passengers and crew, as well as minor damage to the aircraft. Even though none have resulted in major structural failures, the potential should be of concern to airline fleet operators. Although all of these incidents have been attributed to turbulence, it appears that in many of them a significant portion of the *g* load may have come from ensuing aircraft maneuvers. The purpose of this article is to investigate the separation of turbulence and maneuver-induced *g* loads, and in addition, to provide some insight to control problems that arise during clear-air turbulence encounters.

Mechanisms for the development of severe clear-air turbulence are shown in Fig. 1. This figure illustrates the formation of waves and vortices that are associated with air flowing over low-level barriers such as mountains and thunderstorms, and the formation of updrafts above building thunderstorms. Airliners passing in the vicinity of such disturbances can develop large *g* loads. Problems in the control of airspeed and altitude have also been reported by airline pilots, particularly during flight through mountain waves.[1] In mountain waves the large variations in winds can make it difficult for the aircraft to remain in the design envelope between stall and overspeed, and to maintain the assigned altitude. These problems are aggravated by the limited engine thrust available at cruise altitude.

One way to investigate the effects of atmospheric disturbances is through the analysis of airline flight records obtained from turbulence encounters. In conjunction with the National Transportation Safety Board, researchers from Ames have analyzed the series of severe clear-air encounters listed in Table 1. These encounters have involved modern airliners, each equipped with a multichannel digital flight-data recorder (DFDR). (Every airliner certified after 1969 carries a DFDR.) A DFDR records an extensive set of variables which can be used to determine time histories of the winds along the aircraft

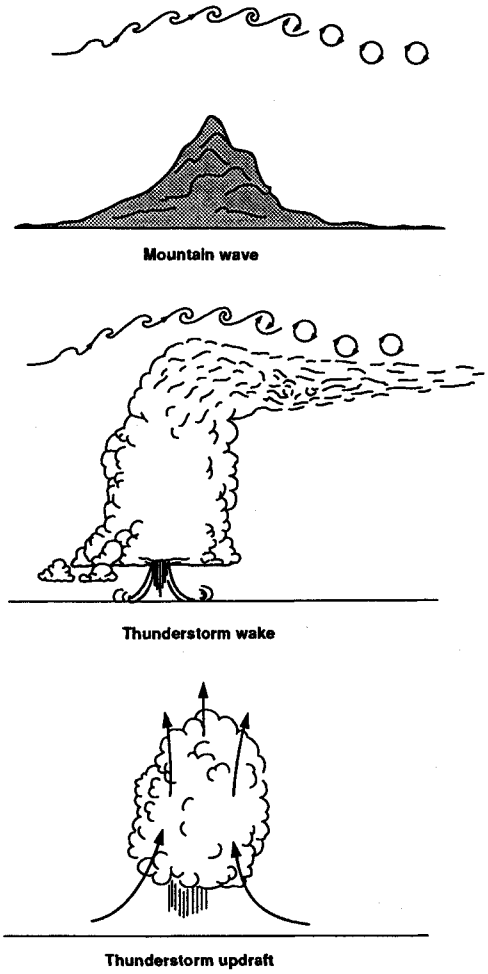

Fig. 1 Mechanisms for the development of severe turbulence.

Presented as Paper 92-4341 at the AIAA Atmospheric Flight Mechanics Conference, Hilton Head, SC, Aug. 10–12, 1992; received Oct. 26, 1992; revision received Feb. 16, 1993; accepted for publication July 3, 1993.

*Aerospace Engineer, Aircraft Guidance and Navigation Branch, Flight Systems and Simulation Research Division. Deceased.
†Aerospace Engineer. Member AIAA.

Table 1 Airline clear-air turbulence incidents involving large g loads

Date				
Month	Day	Year	Location	Altitude, 100 ft
11	3	75	Calgary, Canada	330
4	4	81	Hannibal, MO	370
7	16	82	Morton, WY	390
10	12	83	Bermuda	370
11	25	83	Charleston, SC	330
1	22	85	Greenland	330
4	7	86	Jamestown, NY	400
9	28	87	Bermuda	310
11	11	87	Bermuda	330
3	24	88	Cimarron, NM	330
6	6	89	Garden City, KS	370
8	28	91	Bermuda	290

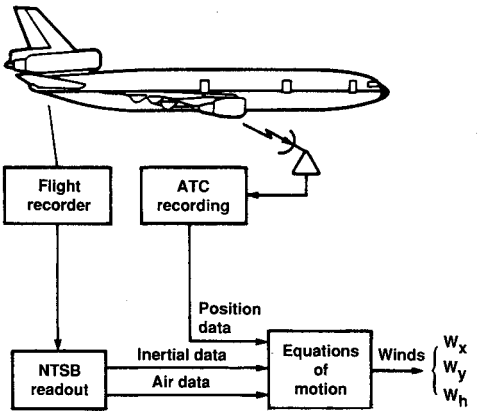

Fig. 2 Estimation of winds from DFDR and ATC records.

flight path.[2] The DFDR also provides the means to separate contributions of aircraft maneuvering to measured g loads, and to analyze problems in aircraft control that arise during atmospheric disturbances.

The DFDR data set includes measurements of specific forces (accelerations), Euler angles, indicated airspeed, temperature, and pressure altitude as well as control-surface positions and engine power. "Discretes" (binary variables), such as landing-gear status (up or down) and microphone keying (on or off) are also recorded. The sampling rate depends on the dynamic nature of the variable: typically, accelerations are sampled 4 or 8 times/s, while engine parameters are sampled only once every 4 s. Most of the other variables are sampled at 1/s. These records, along with (ground) ATC radar or (onboard) GPS/INS position data comprise a measurement set approaching that available from flight test. Therefore, it is possible to determine aircraft performance in turbulence, and to characterize the turbulence environment.

Previous studies[3-7] have presented analyses of the nature and cause of the estimated wind variations for several of the cases listed in Table 1. Here, the flight records for these cases are re-examined to analyze the aircraft response to both turbulence and maneuvering. Short-term variations in elevator deflection and pitch angle are used as guides in separating the turbulence and maneuvering g loads. In addition, the effects of flight-path winds are compared with the countering control actions (pitch angle and thrust) to provide new insight into the dynamics and control problems in mountain-wave flying. The methods used to analyze the flight records are described first. Results from the analysis of turbulence encounters involving waves and vortices are presented, followed by those encounters involving updrafts. Then, examples with significant maneuvering are presented, and the variations in g load for the different sets of cases are compared. Finally, examples of control problems in mountain waves are presented and discussed.

Analysis Methods

Wind Estimation

Figure 2 shows a block diagram of the procedure used to determine time histories of winds along the aircraft flight path.[8] In this analysis the aircraft accelerations are integrated to determine the flight path that provides a best match to the ATC radar position data and the DFDR barometric altitude data. The equations of motion are in an Earth frame with the x axis pointing N, the y axis pointing E, and the h axis vertical (z axis down). The aircraft accelerations are given by

$$\begin{aligned}\ddot{x} &= a_x \cos\theta\cos\psi + a_y(\sin\phi\sin\theta\cos\psi - \cos\phi\sin\psi) \\ &\quad + a_z(\cos\phi\sin\theta\cos\psi + \sin\phi\sin\psi) \\ \ddot{y} &= a_x \cos\theta\sin\psi + a_y(\sin\phi\sin\theta\sin\psi + \cos\phi\cos\psi) \\ &\quad + a_z(\cos\phi\sin\theta\sin\psi + \sin\phi\cos\psi) \\ \ddot{h} &= a_x \sin\theta - (a_y\sin\phi + a_z\cos\phi)\cos\theta - g \end{aligned} \tag{1}$$

where a_x, a_y, and a_z are the body-axis specific forces, and ϕ, θ, and ψ are the body-axis Euler angles. Integration of these differential equations provides estimates of inertial velocity ($\dot{x}$, $\dot{y}$, $\dot{h}$) and position (x, y, h). A set of initial conditions and bias corrections is determined by matching the calculated x and y time histories to ATC radar position data, and by matching the calculated h time history to the DFDR barometric altitude data.

The wind velocity is computed as the difference between the vehicle inertial velocity and its velocity with respect to the air mass. The components of the wind vector are given by

$$\begin{aligned} W_x &= \dot{x} - V\cos\psi_a\cos\gamma_a \\ W_y &= \dot{y} - V\sin\psi_a\cos\gamma_a \\ W_h &= \dot{h} - V\sin\gamma_a \end{aligned} \tag{2}$$

where the true airspeed V is computed from the flight records, and the wind-axis Euler angles γ_a and ψ_a are computed using the identities

$$\begin{aligned} \sin\gamma_a &= \cos\alpha\cos\beta\sin\theta - C\cos\theta \\ \tan(\psi_a - \psi) &= (\sin\beta\cos\phi - \sin\alpha\cos\beta\sin\phi)/D \\ D &= \cos\alpha\cos\beta\cos\theta + C\sin\theta \\ C &= \sin\alpha\cos\beta\cos\phi + \sin\beta\sin\phi \end{aligned} \tag{3}$$

where α is the angle of attack, and β is the angle of sideslip. Methods have been developed to estimate these airflow angles when vane-angle records are not available.[8,9]

Control and Maneuvering

The effect of engine thrust for control in turbulence can be evaluated from the wind-axis performance equation, which is well-approximated in cruise by the expression

$$V/g + \dot{h}/V = (T - D)/W - (\dot{W}_{xy}/g - W_h/V) \tag{4}$$

where T is the thrust directed along the wind axis, D is the drag force, and W is the aircraft weight. The "excess thrust" term is computed from records of specific force and angle of attack as

$$(T - D)/W = a_x\cos\alpha + a_z\sin\alpha \tag{5}$$

where it is assumed that the sideslip angle is negligible ($\beta = 0$). The first wind term within the brackets of Eq. (4) is defined as

$$\dot{W}_{xy} = \dot{W}_x \cos \psi_a + \dot{W}_y \sin \psi_a \qquad (6)$$

which is a time rate of change of horizontal wind along the flight path. The two wind terms in Eq. (4) combine to make up what has become known as the wind shear-hazard index or "F-factor."[10] Thus, in order to maintain stable flight ($\dot{V} = \dot{h} = 0$), the performance equation indicates that the excess-thrust term must be able to follow variations in the F-factor.

The effect of aircraft pitch angle for control in turbulence can be derived from Eqs. (2) and (3), with sideslip again considered negligible, as

$$\dot{h} = V \sin(\theta - \alpha) + W_h \qquad (7)$$

For altitude stabilization ($\dot{h} = 0$), this equation indicates that the term $V \sin(\theta - \alpha)$ must counter variations in the vertical wind term W_h.

Changes in aicraft g load are primarily related to short-term changes in angle of attack. One way to separate the turbulence and maneuver effects in g loading is through analysis of the short-term variations in elevator deflection and aicraft pitch angle. Vertical winds induce changes in α that are independent of θ, but elevator control inputs induce changes in α that are correlated with θ. This can be seen by solving Eq. (7) for α, using a small-angle approximation, to obtain

$$\alpha = (\theta - \gamma) + W_h/V, \qquad \gamma = \dot{h}/V \qquad (8)$$

Note that in the absence of vertical wind, the angle of attack is directly correlated with pitch angle.

It should also be noted that for an aircraft in cruise ($M \approx 0.8$), a wind "up-gust" or a control "pull-up" may cause the wing to enter a stall-buffet region with a relatively small increase in g load. The nonlinear aerodynamics near cruise also mean that a larger (negative) change in g load will occur for the same magnitudes of "down-gust" and "push-down." Negative g load changes can cause injuries to those onboard not secured by seatbelts. These effects will be illustrated in the results presented in the sections that follow.

Results and Discussion

Waves and Vortices

Severe clear-air turbulence can result from the growth and breakdown of stratified shear layers.[11,12] These conditions are typically encountered at altitudes near the tropopause and are often associated with the jet stream. The most severe encounters occur in atmospheric waves that develop with air flowing above mountains and thunderstorms.[13] In 6 of the 12 cases listed in Table 1 the severe turbulence encounters occurred at locations downwind of mountains and thunderstorms. Three of the cases (Cimarron, Calgary, and Morton) were over western mountain ranges, and a fourth case was over mountains in Greenland. The two other cases (Hannibal and Charleston) were in the wakes of thunderstorms.

A representative case is that near Cimarron where an airliner was cruising at 33,000 ft along an easterly track with a prevailing wind from the W. The turbulence encounter occurred as the aircraft passed over the eastern slope of the Sangre de Cristo Mountains. Using the data from the DFDR, the winds along the aircraft track were estimated with the technique described in the previous section. Time histories of these estimated winds along with information from the DFDR are presented in Fig. 3. Note that the horizontal wind increases as the aircraft passes over the mountain range. The deviations in vertical wind indicate both slow variations (mountain waves) and rapid changes (turbulence). The turbulence appears as sudden jolts with load deviations of +0.73 and −1.20 g. Following the encounter, the aircraft made a smooth, controlled descent. In this case, there is no evidence of significant maneuver-induced g loads.

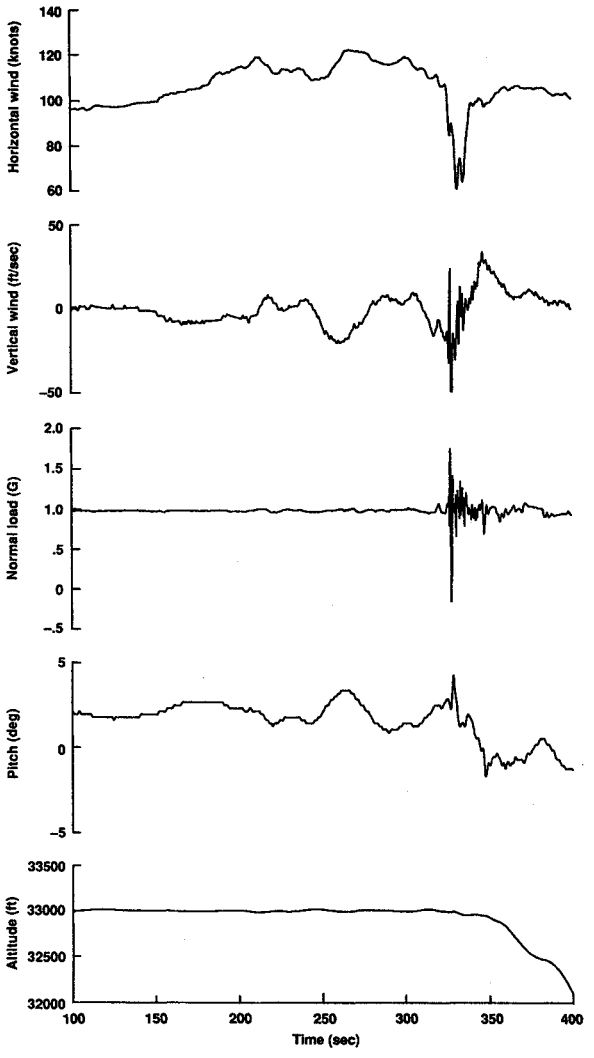

Fig. 3 Flight-path winds and data for the Cimarron case.

	Vortex diameter (feet)	Tangential velocity (ft/sec)
Hannibal	1000	85
Morton	900	70
Cimarron	900	50

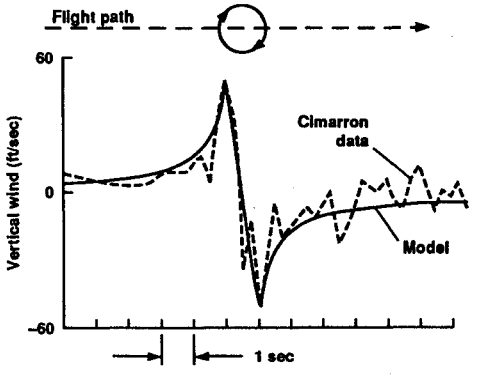

Fig. 4 Models for vortex-induced turbulence.

Previous studies[3,5] have noted that sharp, sudden jolts are often associated with the passage of aircraft through Kelvin-Helmholtz vortices.[11] Identification techniques have been developed to determine the size and strength of the vortices

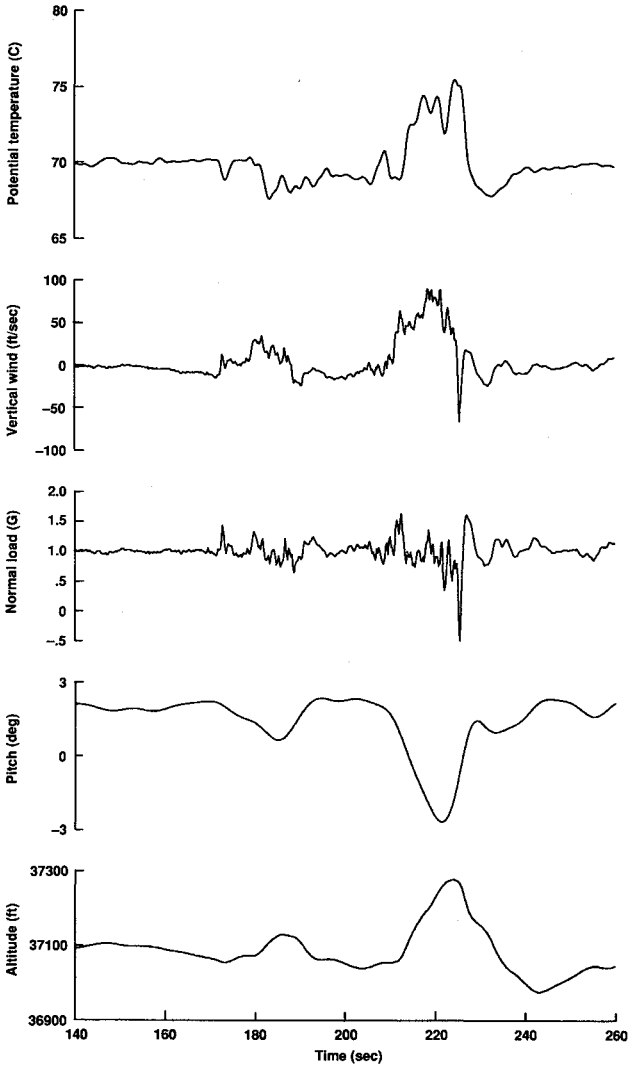

Fig. 5 Time histories for the updraft encounter near Bermuda on 10/12/83.

from the DFDR data.[14] A vortex model for the Cimarron case is presented in Fig. 4. The large spikes in the vertical wind are caused by the passage of the aircraft through the core of the vortex. These spikes provide significant evidence about the size and strength of the vortex wind pattern. Here the vortex core has a diameter of 900 ft and a maximum tangential wind of 50 ft/s. Figure 4 also presents a comparison of vortices determined in previous studies.[3,14] It is seen that the vortex cores have diameters of 900–1000 ft, with tangential winds up to 85 ft/s.

Thunderstorm Updrafts

Severe turbulence can be found in strong updrafts associated with rapidly building thunderstorms.[15] During the initial stage of thunderstorm development there can be updrafts of 50 ft/s, and as the thunderstorm builds, the updrafts can reach values of 100 ft/s. Thunderstorm buildups may not be detected by the onboard weather radar for cases with large vertical winds. (The radar beam may not be tilted down enough or the cloud particles may not be large enough.) In 4 of the 12 cases listed in Table 1 the turbulence occurred in strong updrafts near the tops of building thunderstorms that were not detected by onboard weather radar. These clear-air turbulence incidents occurred on routes from New York that cross the Sargasso sea (SW of Bermuda). They were reported during the months of August–November, which is the season of maximum thunderstorm activity in this region.

A representative case is that near Bermuda on October 12, 1983, in which severe turbulence was encountered as the airliner was cruising in a northerly direction at 37,000 ft. The pilot noted that no precipitation droplets were detected ahead of the aircraft by the onboard weather radar. The pilot did note, however, that the aircraft passed through the top of a cumulus cloud at the time of the encounter. Satellite data do indicate that convective activity existed in the area.[7] The vertical wind and DFDR measurements are presented in Fig. 5. The results show regions of updrafts with vertical winds over 80 ft/s. The changes in vertical wind are positively correlated with changes in air temperature, which is an indication of convective activity.[7] The results show that as the aircraft enters the updraft there is a positive load change of 0.66 g, and as the aircraft exits the updraft there is a negative load change of 1.58 g. Note the variation in pitch angle during the time the aircraft is in the updraft. This is primarily the result of the basic airframe response to an updraft. The amount of pitch variation is a function of the length of time in the updraft and the magnitude of the updraft. In this case, a 20-s encounter with an 80 ft/s-updraft resulted in a 5.2-deg variation in pitch angle. Although there were small elevator inputs during this period, maneuvering did not contribute significantly to the g load.

Turbulence and Maneuver Loads

As indicated in a previous section [see Eq. (8)], one way to separate the turbulence and maneuvering effects on g loading (or angle of attack) is through analysis of the short-term variations in elevator deflection and aircraft pitch angle. Vertical winds induce changes in α that are independent of θ, but control inputs induce changes in α that are correlated with θ. Examples that illustrate both turbulence and maneuver g loads are shown in Fig. 6. In these examples the time histories for g load and angle of attack are given along with the elevator-control deflection. Also, the pitch-angle term from Eq. (8) is superimposed on the angle-of-attack time histories.

The results for the vortex encounter near Cimarron are presented again in Fig. 6a. During the encounter the small changes in the aircraft pitch angle are consistent with a previous simulation study[5] that indicates how different aircraft will tend to follow changes in vertical wind. The actual data show that initially the aircraft pitches down ($\Delta\theta = -0.5$ deg) in response to the positive vertical wind, and then as vortex core is traversed, the aircraft pitches up ($\Delta\theta = +1.8$ deg) in response to the negative vertical wind. Subsequently, a small amount of elevator control is applied to bring the pitch angle down. The small pitch-angle changes during the vortex encounter represent the basic airframe response to turbulence, and are not caused by maneuvering.

The time histories for the Calgary case shown in Fig. 6b illustrate a sharp pitch-down maneuver that was used to initiate a controlled descent following a brief turbulence encounter.[4] Note that the downward movement in elevator control is correlated with changes in g load, α, and $(\theta - \gamma)$. Following the initial pitch down, there are short oscillations in the elevator control that are correlated with changes in the same variables. The correlation among these variables indicates a major influence of maneuvering on the large negative g loads induced during this time segment.

Other examples that involve large maneuvering g loads are presented in Fig. 7. The two cases that are compared in Fig. 7a (Jamestown and Garden City) are similar. In each case there was an increasing headwind (not shown), and in response to this (airspeed increase) there was a corresponding increase in pitch angle. The pitch angle was increasing with positive angular momentum as the aircraft entered the stall-buffet region, and because of the nonlinear pitching moment, there is a natural tendency for the pitch angle to increase even further. Subsequently, in response to the increased pitch angle, g load, and buffet, there are sharp pushdowns in the elevator controls with rapid pitch-angle changes to -12 deg, and negative loads to -1.92 g. These pitch downs are then followed by damped oscillations of the

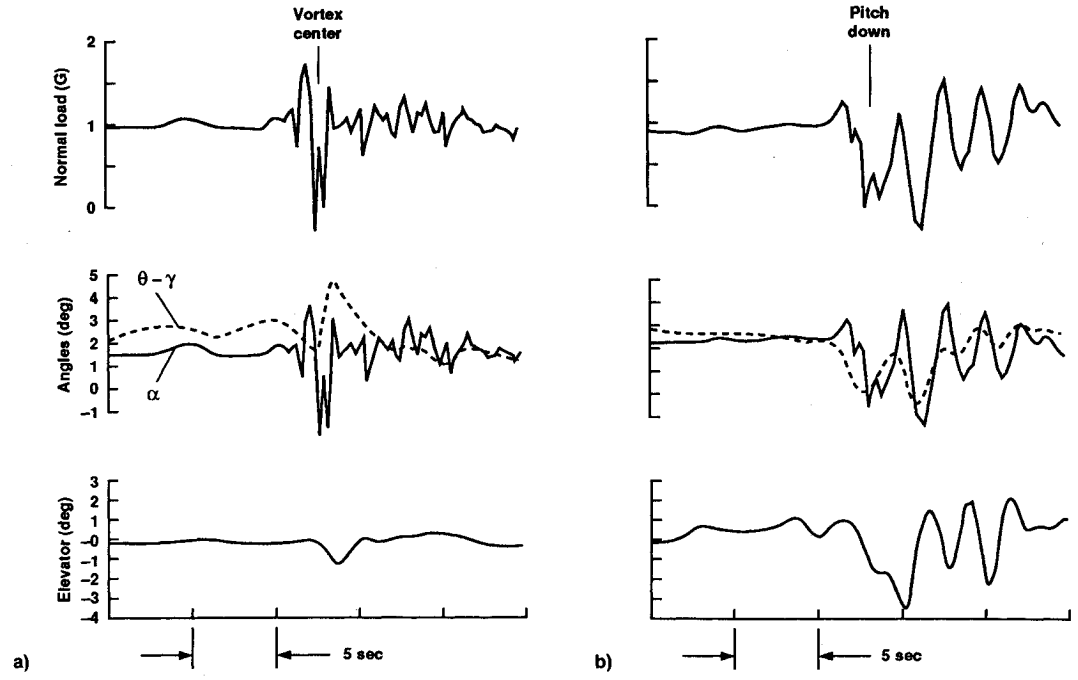

Fig. 6 Comparison of turbulence and maneuvering g loads: a) vortex encounter in Cimarron case and b) pitch-down maneuver in Calgary case.

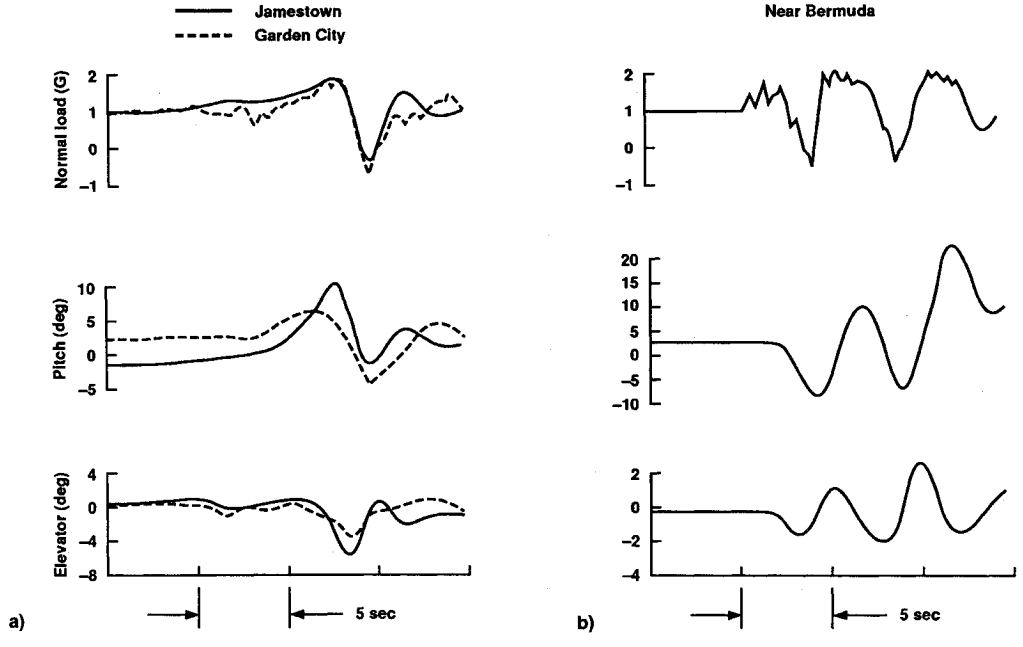

Fig. 7 Comparison of cases with significant maneuvering: a) Jamestown and Garden City and b) near Bermuda on 11/11/87.

Table 2 Extreme value of load increments (g units) for turbulence encounters

Date				Waves		Updrafts		Maneuvering	
Month	Day	Year	Location	Max	Min	Max	Min	Max	Min
11	3	75	Calgary	+0.63	−0.75	—	—	—	−1.22
4	4	81	Hannibal	+0.78	−1.99	—	—	+0.83	—
7	16	82	Morton	+0.67	−1.62	—	—	—	—
10	12	83	Bermuda	—	—	+0.66	−1.58	+0.59	—
11	25	83	Charleston	+1.09	−2.01	—	—	—	—
1	22	85	Greenland	+1.70	−0.95	—	—	—	—
4	7	86	Jamestown	—	—	—	—	+0.84	−1.35
9	28	87	Bermuda	—	—	+1.17	−1.53	—	—
11	11	87	Bermuda	—	—	+0.69	—	+0.99	−1.61
3	24	88	Cimarron	+0.73	−1.20	—	—	—	—
6	6	89	Garden City	—	—	—	—	+0.98	−1.92
8	28	91	Bermuda	—	—	+0.95	−1.69	+0.90	—

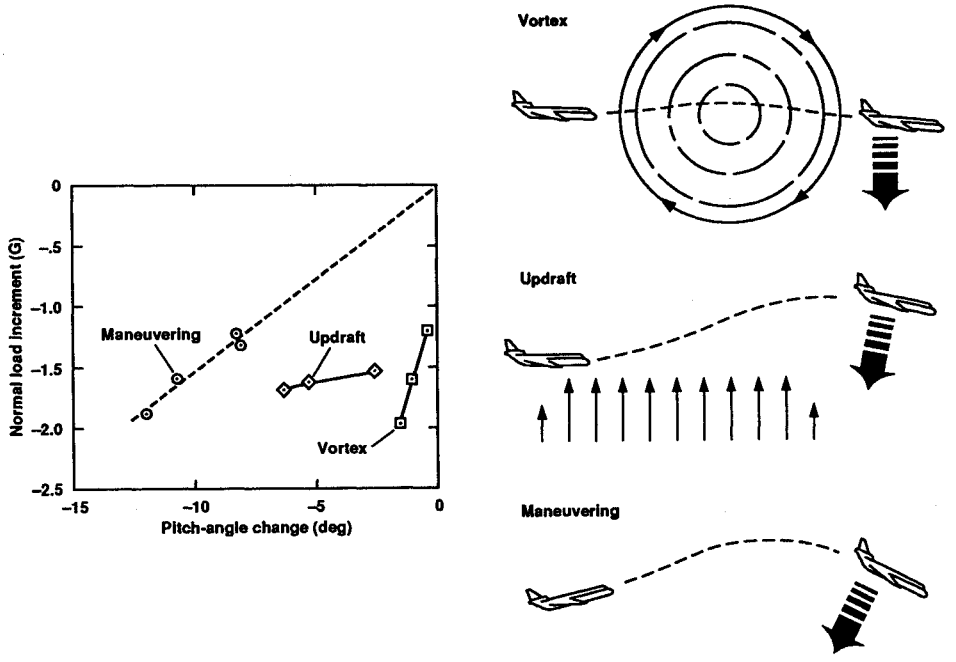

Fig. 8 Comparison of negative changes in pitch angle and g load.

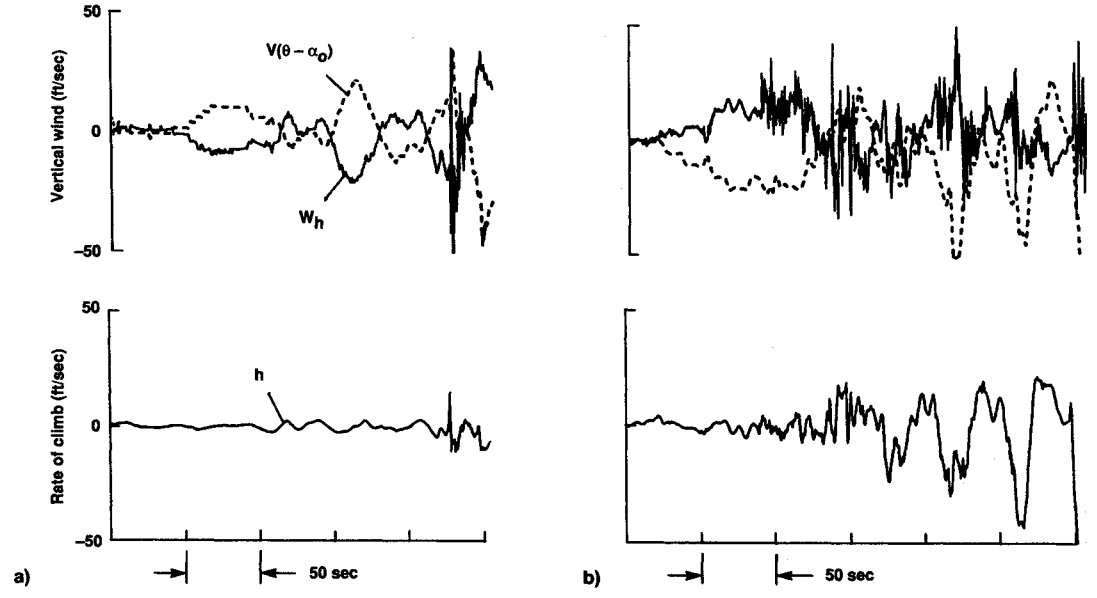

Fig. 9 Comparison of altitude control for two mountain wave cases: a) Cimarron and b) Calgary.

pitch angle in response to correlated movements in the elevator control inputs.

Another case of large g loads (near Bermuda) is shown in Fig. 7b. In this case the aircraft encountered a strong updraft which caused the autopilot to disengage. Subsequently, there is a sharp pushdown in the elevator control with a rapid pitch-angle change of -8 deg. This is followed by oscillatory movements in the elevator control, resulting in large oscillations in pitch angle and g load. The period of oscillation is about 5 s, which is the natural short period of the aircraft. The magnitudes of the positive changes in g load are less than the magnitudes of the negative changes, because of the nonlinear aerodynamics near the stall-buffet region.

Comparison of g Loads

Table 2 presents the extreme load values from the DFDR data for all 12 cases listed in Table 1. As noted earlier, in six of the cases severe turbulence is encountered in waves at locations downwind of mountains and thunderstorms. For these cases the data show (in response to turbulence) positive load changes to 1.70 g and negative load changes to 2.01 g. In four other cases severe turbulence is found to be associated with updrafts in building thunderstorms that were not detected by the onboard weather radar. The data show positive load changes in 1.17 g during the initial encounter with the updraft, and then negative load changes to 1.69 g during the exit from the updraft. As also discussed, there can be g loads from both atmospheric turbulence and maneuvering. The data indicate positive maneuvering loads in six cases, and negative maneuvering loads in four cases. Results show pull-up maneuvers with positive load changes to 0.99 g, and push-down maneuvers with negative load changes to 1.92 g.

As mentioned earlier, negative g loads cause the more severe injuries, particularly to passengers and crew that are not in seatbelts. The clear-air turbulence cases presented here, from reported incidents, all show large values of negative g loads. These large negative loads are associated with distinct patterns in the pitch-angle variations for different sets of cases. A summary comparison of the changes in negative load and pitch angle is presented in Fig. 8. The data points shown on this figure are the maximum *negative* changes

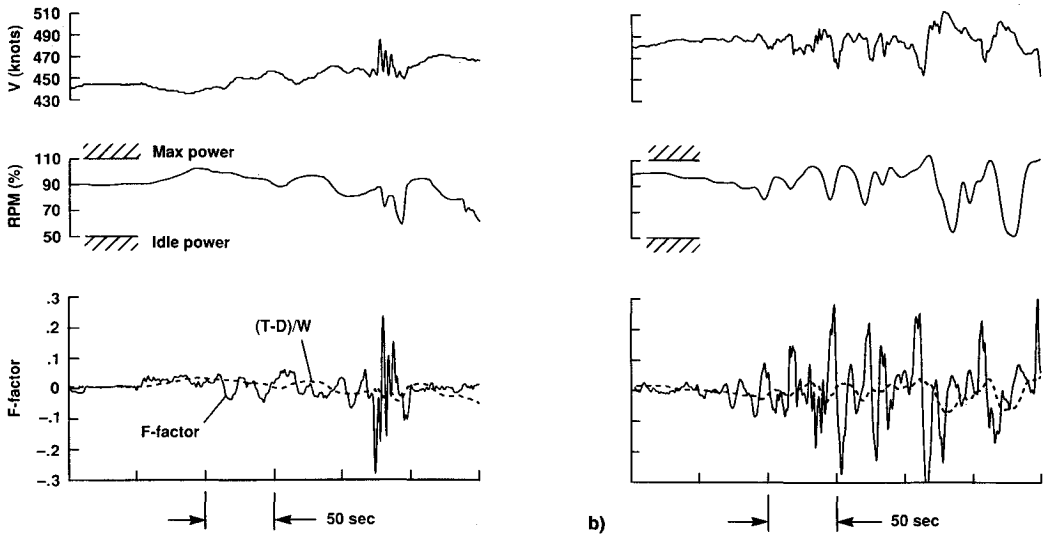

Fig. 10 Comparison of airspeed control for mountain wave cases (lower curves are 5-s moving averages): a) Cimarron and b) Calgary.

in each of the categories involving vortices, updrafts, and maneuvering.

For each case involving vortex encounters there is a relatively small change in pitch angle. The change is small because of the large pitch moment-of-inertia of the aircraft and the short time required to traverse the vortex. In the extreme case there is only a change in pitch angle of 1.4 deg for a change in load of 1.99 g. For an updraft encounter there is typically a larger decrease in pitch angle. The longer duration of this type of encounter allows the aircraft to "weather-cock" in response to changes in vertical wind. For the extreme case there is a change in pitch angle of 6.2 deg, and a change in load of 1.69 g. For the maneuvering cases there are large changes in pitch angle with corresponding large changes in the g load. Note the good correlation between the magnitudes of the changes in pitch angle and g load. In the extreme case there is a change in pitch angle of 12 deg and a deviation in load of 1.92 g.

Altitude and Airspeed Control

The avoidance of atmospheric disturbances is important not only to reduce conditions leading to large g loads, but also to reduce problems in control of altitude and airspeed. In mountain waves the control of altitude and airspeed can be particularly challenging, as described in a recent airline pilot comment.[1]

> . . . a mountain wave can take an aircraft through rapid changes in temperature, Mach, and relative wind, literally in a matter of a few seconds. From near stall condition to . . . (overspeed) . . . and quickly back can be terrifying. The crew and/or the autoflight system must try to compensate, and rapidly or risk possible stall or upset and displacement from assigned cruising altitude before recovery.

In this section, it is shown how records from the aircraft DFDR can be used to provide insight into the control problems involved in turbulence encounters.

Figure 9 presents a comparison of altitude control in the Cimarron and Calgary cases. This figure presents time histories of altitude rate and vertical wind. Superimposed on the trace of W_h is the term $V \sin(\theta - \alpha_0)$ from Eq. (7), where α_0 represents a nominal trim value. In the Cimarron case the results show that the pitch angle varies appropriately to counter variations in the vertical wind in order to minimize deviations in altitude rate. In the Calgary case the pitch angle is shown to vary in proper proportion to the longer-period (120-s) variations in the vertical wind, but at a shorter 40-s period, the changes in pitch become out of phase, intensifying the deviations in altitude rate. The phasing problem arises because the pitch angle is being used to control both altitude and airspeed. The results indicate that reasonable pitch angle changes (e.g., ± 3 deg) are sufficient to counteract the vertical winds (e.g., ± 50 ft/s). However, it is important that these pitch angle changes be properly timed in order to minimize the deviations in altitude.

Figure 10 presents a comparison of airspeed control in the Cimarron and Calgary cases. The upper curves show the variations in airspeed and engine rpm. As in most cases, the engines are varied inversely in proportion to changes in airspeed, and the magnitudes of the variations in engine power are quite large. As shown, the engine rpm varies through extremes from 50% (near idle power) to 110% (near max power). The lower curves present the specific force $(T - D)/W$ along with the windshear-hazard index [F-factor in Eq. (4)]. The results show that the F-factor varies sharply, with extreme values outside the range ± 0.2. (These F-factor magnitudes are on the order of the largest found with microbursts near the ground.[10]) The primary contribution to the F-factor in mountain waves, for aircraft with large airspeed, is the time derivative of the horizontal wind W_{xy}. As shown, the magnitude of the changes in $(T - D)/W$ are not large enough to counter the deviations due to the winds. Also, the timing of the changes in thrust is lagged by many seconds. In the Calgary case this lag in engine response is associated with a dynamic instability in airspeed control.

Previous studies of airliners in severe turbulence have noted the problems of controlling airspeed using variations in either pitch angle or engine power.[16,17] These studies of jet upsets have suggested that in severe turbulence the pitch angle deviations should be loosely held within reasonably small limits (e.g., ± 3 deg) and the engine power should be held constant. Difficulties with this standard operating procedure arise in strong atmospheric waves, however, when there are large deviations in airspeed. Further study is warranted to provide the best combination of pitch and engine feedbacks in severe atmospheric disturbances, particularly to insure dynamic stability. Energy management concepts[17,18] might provide the means to blend the pitch and engine feedbacks.

Concluding Remarks

In this article digital flight records from airline clear-air turbulence encounters have been used to determine winds along the aircraft flight path, to determine maneuver g loads, and to analyze control problems. Results have been presented from 12 reported turbulence incidents that have been analyzed to date.

In six of the cases severe turbulence is encountered at locations downwind of mountains and thunderstorms. During these encounters, sharp, sudden jolts are found associated with the passage of aircraft through Kelvin-Helmholtz vortices. It is found that the vortex cores have diameters of 900–1000 ft, with tangential winds up to 85 ft/s. In response to the vortex-induced turbulence, the results show load changes of $+1.70$ and -2.01 g.

In four other cases severe turbulence is found to be associated with updrafts above building thunderstorms that were not detected by onboard weather radar. These updrafts (all near Bermuda) are found to be quite strong, with vertical winds over 80 ft/s. The data show pitch-angle changes of -6 deg in response to these strong updrafts. Results show load changes to $+1.17$ g during entry to the updraft, and load changes to -1.69 g during exit from the updraft.

An important finding is that there are large maneuvering loads in over half of the reported clear-air turbulence incidents. Maneuvering g loads are determined through an analysis of the short-term variations in elevator deflection and aircraft pitch angle. The magnitudes of the negative load changes caused by maneuvering are found to be significant. Results show sharp pushdowns with pitch angle changes to -12 deg with corresponding load changes to -1.92 g.

For altitude control in mountain waves the results indicate that reasonable pitch angle changes (e.g., ± 3 deg) are sufficient to counter the vertical winds, and thus maintain level flight. However, it is important that these pitch angle changes be timed appropriately. In mountain waves the magnitudes of the variations in F-factor (windshear hazard index) are found to be quite large. The results indicate that at cruise altitudes there is neither the available thrust nor the quickness in engine response necessary to counter the large and rapid variations in horizontal wind.

Acknowledgments

The authors thank Peter Lester of San Jose State University, San Jose, California, for his valuable contributions in meteorological analysis for these case studies, and they thank the staff at the National Transportation Safety Board, Washington, D.C., for their aid in obtaining the data used in this report.

In Memoriam

Rodney Wingrove died on April 22, 1992, following a brief illness. After earning the BSAE degree from the University of Washington in 1955, Rodney joined the staff at NASA Ames Research Center. He first became known for his definitive work in spacecraft re-entry optimization, and later for his contributions in the area of aircraft state and parameter estimation. In recent years his research was directed toward aircraft accident analysis and the effects of atmospheric disturbances on aircraft operation. He is sorely missed by his many friends and colleagues.

References

[1]Stack, D. T., "Turbulence Avoidance," *Proceedings of the 4th International Conference on Aviation Weather Systems*, American Meteorology Society, Boston, MA, 1991, pp. 283–286.

[2]Bach, R. E., and Wingrove, R. C., "Application of State Estimation in Aircraft Flight-Data Analysis," *Journal of Aircraft*, Vol. 23, No. 7, 1985, pp. 547–554.

[3]Parks, E. K., Wingrove, R. C., Bach, R. E., and Mehta, R. S., "Identification of Vortex-Induced Clear Air Turbulence Using Airline Flight Records," *Journal of Aircraft*, Vol. 22, No. 2, 1985, pp. 124–129.

[4]Lester, P. F., and Bach, R. E., "An Extreme Clear Air Turbulence Incident Associated with a Strong Downslope Windstorm," AIAA Paper 86-0329, Jan. 1986.

[5]Wingrove, R. C., Bach, R. E., and Schultz, T. A., "Analysis of Severe Atmospheric Disturbances from Airline Flight Records," AGARD CP-470, May 1989, pp. 3-1–3-7.

[6]Lester, P., Sen, O., and Bach, R. E., "The Use of DFDR Information in the Analysis of a Turbulence Incident over Greenland," *Monthly Weather Review*, Vol. 117, June 1989, pp. 1103–1107.

[7]Pantley, K. C., and Lester, P. F., "Observations of Severe Turbulence Near Thunderstorm Tops," *Journal of Applied Meteorology*, Vol. 29, Nov. 1990, pp. 1171–1179.

[8]Bach, R. E., and Wingrove, R. C., "Analysis of Windshear from Airline Flight Data," *Journal of Aircraft*, Vol. 26, No. 2, 1989, pp. 103–109.

[9]Bach, R. E., and Parks, E. K., "Angle-of-Attack Estimation for Analysis of Wind Shear Encounters," *Journal of Aircraft*, Vol. 24, No. 11, 1987, pp. 789–792.

[10]Bowles, R. L., and Targ, R., "Windshear Detection and Avoidance: Airborne Systems Perspective," *Proceedings of the 16th Congress of ICAS*, 1988, pp. 7–20.

[11]Scorer, R. S., *Environmental Aerodynamics*, Wiley, New York, 1978.

[12]Gossard, E. E., and Hooke, W. H., *Waves in the Atmosphere*, Elsevier, New York, 1975.

[13]Hopkins, R. H., "Forecasting Techniques of Clear Air Turbulence Including that Associated with Mountain Waves," World Meteorological Organization TN 155, 1976.

[14]Mehta, R. S., "Modeling Clear-Air Turbulence with Vortices Using Parameter Identification Techniques," *Journal of Guidance, Control, and Dynamics*, Vol. 10, Jan. 1987, pp. 27–31.

[15]Kessler, E. (ed.), "Thunderstorms: A Social, Scientific, and Technological Documentary," *Thunderstorm Morphology and Dynamics*, Vol. 2, Univ. of Oklahoma Press, Norman, OK, 1985.

[16]Caiger, B., "Review of Several Factors Relevant to Jet Upsets," AGARD CP-76, 1970, pp. 14-1–14-9.

[17]Johnson, D. E., Klein, R. H., and Hoh, R. H., "Manual and Automatic Flight Control During Severe Turbulence Penetration," NASA CR 2677, April 1976.

[18]Lambregts, A. A., "Vertical Flightpath and Speed Control Autopilot Design Using Total Energy Principles," AIAA Paper 83-2239, Aug. 1983.